Electrostatically excited liquid marble as a micromixer

ARTICLE

Electrostatically excited liquid marble as a micromixer

Nhat-Khuong Nguyen,[a] Pradip Singha,[a] Hongjie An,[a] Hoang-Phuong Phan,[a] Nam-Trung Nguyen*[a] and Chin Hong Ooi*[a]

Received 00th January 20xx,
Accepted 00th January 20xx

DOI: 10.1039/x0xx00000x

Liquid marble is a promising microfluidic platform for microreactor applications. However, the lack of contactless and on-demand mixing strategies significantly hinders its potential. This paper reports the use of electrostatic force as an actuation scheme to induce vibration and deformation in a liquid marble, thus enhancing the internal flow and promoting mixing in this platform. The effect of a uniform AC electric field on liquid marbles with different volumes was investigated. The results show significant improvement in mixing performance when the liquid marbles were actuated. Increasing electric field strengths also substantially enhances the mixing process. These results show the potential of using a liquid marble as a high-performance micromixer by exploiting the mechanisms of vibration and deformation.

1. Introduction

Microfluidics, the interdisciplinary technology dealing with the manipulation of liquid on the microscale, recently attracted a great deal of attention from the research community.[1] Microfluidics-based devices serve as reliable platforms for a range of biological and chemical applications.[2-5] Furthermore, the advancement of microfabrication enables the development of various microfluidic devices with microscale features.[6] To date, continuous-flow microfluidics attracts a huge interest due to their apparent advantages compared to conventional platforms, particularly for microreactor and micromixer.[1, 7-9] For microreactor applications, the small size of continuous-flow microfluidic devices reduces the amount of reagents and waste and enhances reaction efficiency.[10, 11] Continuous-flow micromixers promote mixing by inducing chaotic advection or disturbances.[10, 12-14] Nevertheless, the difficulties in handling a minute amount of liquid and the stable laminar flow significantly limit the potential of continuous-flow microfluidic devices. For instance, wetting of the device walls leads to mass loss and cross-contamination.[15] Furthermore, if reactions involve solid particles or precipitates, microfluidic devices could be clogged.[16, 17]

Liquid marbles are droplets packaged within a shell of micro- or nanoparticles, and have been gaining great research interest over the last decade.[18, 19] Liquid marble is a digital microfluidic platform owing to its ability to serve as a manipulation platform for individual droplets.[19] In addition, a liquid marble can sustain large and reversible deformation of up to 30%,[20-22] thus by its nature is a digital micro elastofluidic platform.[23] Furthermore, the facile fabrication process and numerous superior characteristics significantly increased the potential of liquid marbles. Liquid marble can be produced simply by rolling a droplet on a powder bed.[24] Recent studies demonstrated new methods to generate liquid marbles automatically using gravitational force,[25] centrifugal force,[26] and electrostatics.[27-29] The coating shell allows liquid marbles to behave like a soft solid that has negligible wetting even with hydrophilic solid surfaces.[30-33] The encapsulating layer effectively eliminates direct physical contact between the interior liquid and the surrounding environment, thus reducing evaporation as well as avoiding contamination and loss of mass due to surface wetting.[30, 34] Recent studies showed that liquid-marble-based microreactors can conveniently accommodate a broad range of reactions involving different reaction kinetics and phases.[19, 35-37] Liquid marbles are also highly versatile in terms of size and responsiveness to external stimuli.[38] These properties make liquid marbles an excellent candidate for a microreactor.

On the other hand, the lack of an effective mixing method considerably limits the potential of a liquid-marble-based microreactor. Mixing plays an extremely important role in microreactors, such as enhancing heat and mass transfer, which in turn improves reaction efficiency.[10] For biological applications, mixing enables the dispersion of nutrient and waste products, which is crucial for cell culture.[39] Particularly, Liu et al. reported that reaction yield can be increased by two times with sufficient mixing.[40] However, mixing in microfluidic platforms remains a challenge due to the prevalent laminar flow in microscale devices, thus necessitating the introduction of external stimulation to induce mixing.[41] In previous studies, mixing was induced by moving a liquid marble under a magnetic field.[36] However, this method is only applicable to liquid marbles with a magnetic coating or dispersed magnetic particles in the liquid and requires manual control. An automated and on-demand mixing strategy that is independent of the type of coating is highly desirable. The feasibility of performing continuous mixing using electrostatic force was also reported.[40, 42] Nevertheless, the direct contact between the electrode and the liquid marble makes the liquid susceptible to contamination. Previous studies demonstrated the feasibility of using external

[a] Queensland Micro- and Nanotechnology Centre, Griffith University, 170 Kessels Road, Nathan 4111 Queensland, Australia
E-mail: nam-trung.nguyen@griffith.edu.au, c.ooi@griffith.edu.au

disturbance such as acoustic wave, [43, 44] electrostatics, [45] or thermal gradient [46] to generate vibration in droplets or liquid marbles, which in turn could induce mixing. Bormashenko et al. first reported a profound deformation of liquid marble in a uniform AC electric field.[47] Recent studies also reported the use of electrostatic force for moving and deforming a liquid marble, and mixing in an on-demand and contactless manner.[48-53] In this study, we investigated the use of an electric field to deform liquid marbles. We expect the deformation will promote mixing by inducing internal flow. Furthermore, the functionality in handling dispersed solid suspension in liquid marble was demonstrated.

2. Theoretical background

For a stationary droplet, mixing mainly occurs through the diffusion process, which is driven by a concentration gradient. Generally, diffusion is slow, and the diffusion rate decreases over time as the concentration gradient decreases. Furthermore, diffusion of bioparticles such as cells is not efficient due to their relatively large size and consequently low diffusivity. For instance, it takes 100 to 1,000 seconds for a molecule with a diameter of 1 to 10 µm to diffuse a distance of 100 µm.[54] Thus, it is necessary to introduce external actuation to enhance mixing performance. Subjected to external actuation, a droplet can be excited to oscillate.[34] Deformation of the droplet usually synchronises with the source of vibration.[55-57] Particularly, in a varying electric field, a droplet can be polarised and vibrated periodically. Under a sufficiently strong electric field, the excited droplet can experience significant deformation or even break up.[58] Previous studies show that the maximum vibrating amplitude of a water droplet can be achieved at resonance, which matches its natural frequency.[44, 55, 59] Similar behaviour was also reported on liquid marbles under electrostatic excitation. In particular, Bormashenko et al. demonstrated and elucidated the deformation of liquid marble under a uniform electric field.[47, 51-53] By applying an external AC electric field to excite a liquid marble at its resonance, we expect the mixing performance to significantly improve due to the convective flow induced by the vibration and deformation of the liquid marble. As the oscillation amplitude increases remarkably at resonance, we expect that the induced flow inside the liquid marble is sufficient to substantially enhance mixing performance.[55]

An AC electric field applied to a droplet or liquid marble generates electric charges that induce Maxwell stress, which in turn induces an electrical force acting on the droplet or liquid marble surface. While the sign of the induced charge changes in harmony with the AC electric field, Maxwell stress always acts outward from the droplet and is proportional to the square of the field strength or the applied voltage. The oscillation frequency is therefore exactly twice the input frequency.[59-62] To achieve resonance, the oscillation frequency should match with the natural frequency, thus the input frequency should be half of the natural frequency of the liquid marble.

3. Materials and Methods

3.1. Preparation of liquid marbles

Liquid marbles reported in this study were formed by dispensing deionised water droplets onto a powder bed of hydrophobised fumed silica (AEROSIL® R 106, ≥ 99.8 % silica, Evonik) using a micropipette and rolled around gently to cover the entire droplet with silica particles. The formed liquid marble appears to be transparent due to the nanometer-sized silica particles as reported in previous studies.[38, 63, 64] The liquid marble was then transferred onto a polymethyl methacrylate (PMMA) substrate under an electrode to be excited. We investigated liquid marbles with volumes of 10, 20, and 40 µL.

3.2. Determination of the natural frequencies of liquid marbles

The liquid marbles were vibrated at their natural frequencies to maximise the deformation and correspondingly mixing. As such, natural frequencies were determined by examining the free vibration of the liquid marbles. We placed the liquid marble under a metal electrode positioned in a PMMA housing with the bottom end exposed. The top end of the electrode was connected to a high voltage power supply of 2.76 kV. When the liquid marble was being deformed by the electrostatic force, the electric field was abruptly removed to allow the liquid marble to vibrate freely. The free vibration of the liquid marble was then recorded using a high-speed camera (Photron FastCam SA3) at a rate of 1,000 frames per second. The recording was subsequently analysed frame by frame using MATLAB. The height of the marble in each frame was determined using the "BoundingBox" function. The natural frequency was found by assessing the periodic change of the height of the liquid marble during the free vibration. Resonance frequencies of liquid marble with volumes 10, 20 and 40 µL were determined and used in subsequent experiments.

3.3. Determination of deformation of liquid marbles

To study the deformation under a uniform AC electric field, liquid marbles with volumes of 10, 20 and 40 µL were placed between two parallel circular metal plates. The parallel plates have a diameter of 55 mm with the top plate connected to a high-voltage power source, whereas the bottom plate was grounded. We kept the distance between the parallel plates constant at 8.5 mm. A PMMA disc with a thickness of 3 mm was placed on the bottom plate to prevent arcing, Figure 1(A). The dielectric constants of PMMA and air were taken as 3 and 1, respectively.[65] Another set of experiment was conducted to investigate the effect of output voltage, V_o, on the deformation of a liquid marble, with voltages of 1, 2, and 2.5 kV applied between the plates. The voltage between the top of the PMMA disc and the top plate, V, is calculated as follow:

$$V = V_0 \frac{\varepsilon_1 d_2}{\varepsilon_2 d_1 + \varepsilon_1 d_2} \quad (1)$$

where ε are the relative permittivities and d are the thicknesses of the components as shown in Figure 1(B). Subscripts 1 and 2 refer to the PMMA and the air gap, respectively. The output voltages of 1, 2, and 2.5 kV thus correspond to the electric field strength of 153, 308, and 385 kV/m, as determined by the equation:

$$E = \frac{V}{d_2} \quad (2)$$

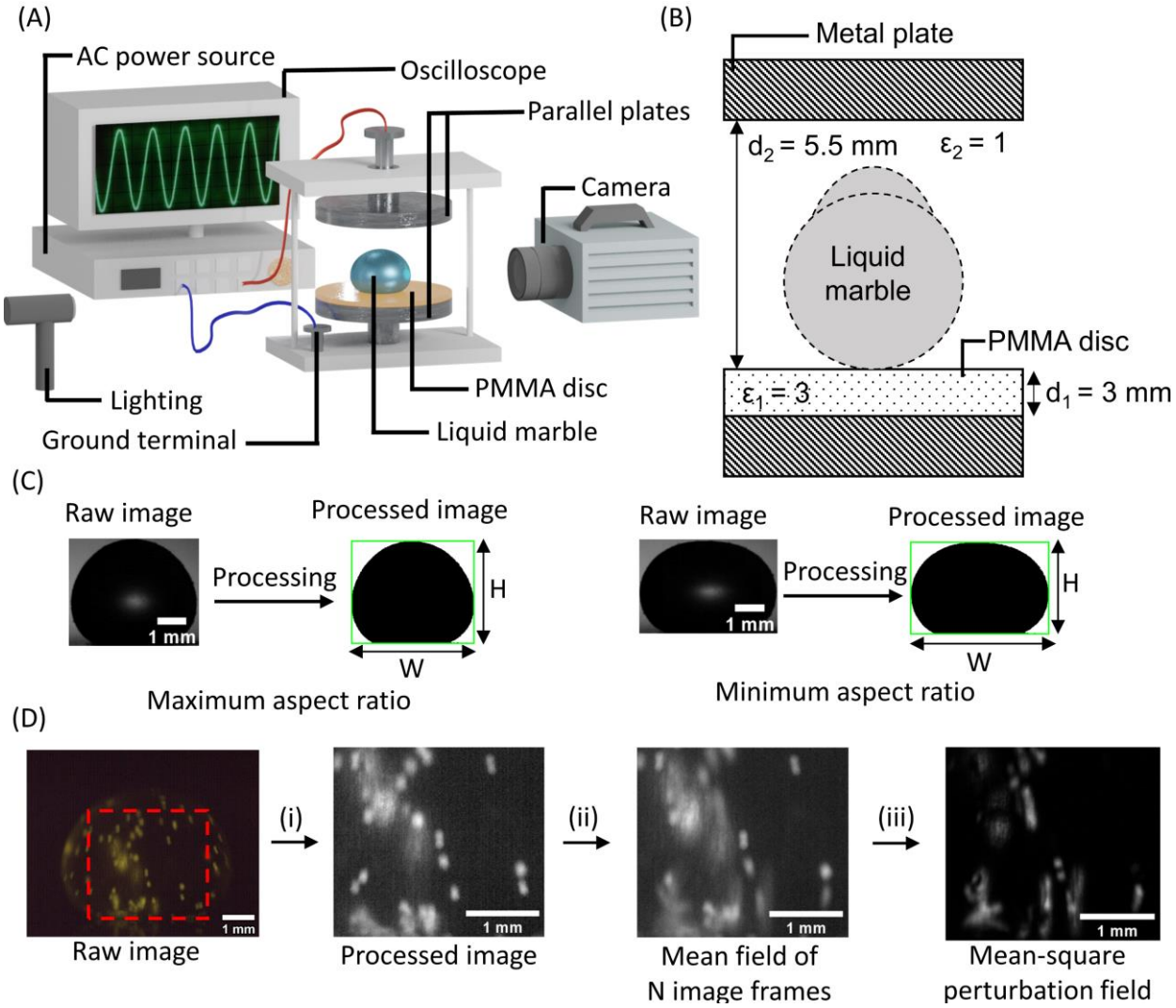

Figure 1. Experimental setup and image analysis for the investigation of the deformation and mixing performance of liquid marble under an AC electric field: (A) Experimental setup;(B) Schematic of the parallel plates; (C) Determining the aspect ratio of liquid marble during vibration; (D) Evaluating the mixing performance in liquid marble by analysing the mean-square perturbation field. (i) Selecting the region of interest (ROI) and converting the image into normalised grayscale. (ii) Calculating the mean fields of N image frames. (iii) Taking the mean-square perturbation field from the mean field of N image frames.

where *E*, *V*, d_2 are the electric field strength, the voltage and the distance between the top of the PMMA disc and the top plate, respectively. The output voltage and waveform were constantly monitored with an oscilloscope. After placing the liquid marble into its position, a uniform AC electric field with a frequency equal to half of the natural frequency of the liquid marble was introduced. The vibration and deformation of the liquid marble were recorded using the same camera setup as in the previous experiment.

The height and width of the liquid marble in each frame was determined using MATLAB as shown in Figure 1(C). The aspect ratio was defined by the following equation:

$$AR = \frac{H}{W} \quad (3)$$

where AR is the aspect ratio and *H* and *W* are the height and width of the liquid marble. The change from a prolate to an oblate shape during vibration was used to evaluate the degree of deformation. Herein, we define the relative deformation *D* as the ratio between these two aspect ratios:

$$D = \frac{AR_{max}}{AR_{min}} \quad (4)$$

where *D* is the relative deformation and AR_{max} and AR_{min} are respectively the maximum and minimum aspect ratio of a liquid marble during vibration.

3.4. Determination of mixing performance in a liquid marble

To study the mixing effect induced by electric actuation, green fluorescent particles (polyethylene microspheres, 1.00 g.cc^{-1}, used as received from Cospheric) with nominal diameters ranging from 90 to 105 µm were dispersed in water as the working liquid. The density of the particle was chosen to match

that of water to minimise gravitational effects. While the fluorescent particles show limited movement without actuation, they can be dispersed throughout the liquid marble if there is sufficient excitation, thus allowing for the study of the mixing effect. The same parallel plates setup and voltage configurations were used to excite the liquid marble. The effect of mixing in a liquid marble was studied using a colour camera (Ximea xiQ - USB3 MQ013CG-ON) and a telecentric lens (Edmund Optics 58430, 1X). A frame rate matching the oscillation frequency was used to record only the motion of the fluorescent particles relative to the liquid marble, creating a stroboscopic effect. Blue light with a peak wavelength of 450 nm was used to illuminate the fluorescent particles within the liquid marble and a longpass filter was placed before the camera lens to remove the blue light.

We processed the recorded images with MATLAB as shown in Figure 1(D). Mixing performance was evaluated by analysing the perturbation field.[13, 66] Since this is a time-dependent process, a single image provides insufficient information with regards to mixing performance. The degree of perturbation was assessed by analysing several image frames over a fixed period of 8.5 seconds. First, a region of interest (ROI) with an area of 450x500 pixel was selected and the normalised intensity was calculated. The normalised intensity or I^* of each image frame was calculated as follows:

$$I^* = \frac{I - I_{min}}{I_{max} - I_{min}} \quad (5)$$

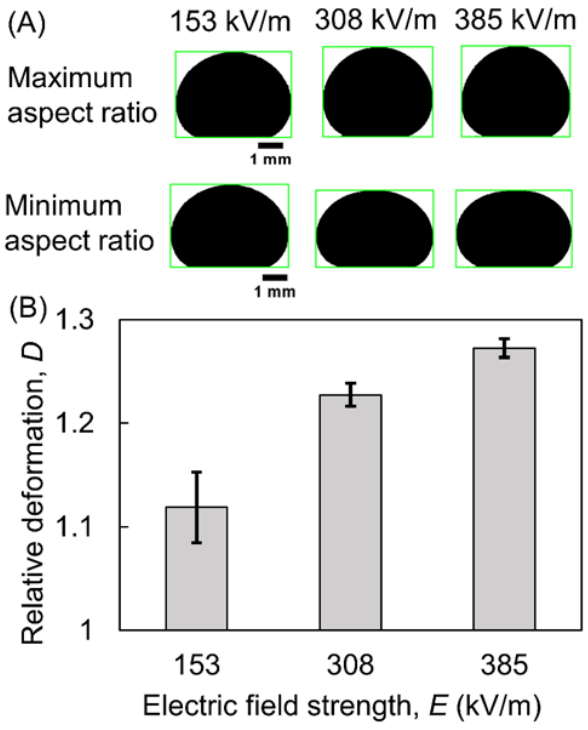

Figure 2. The deformation of liquid marbles at resonance under different electric field strengths: (A) Profile of a 40-µL liquid marble at AR_{max} and AR_{min} with an electric strength of 153, 308 and 385 kV/m; (B) The resultant relative deformation of liquid marbles versus electric field strength.

where I_{max} and I_{min} are the maximum and minimum intensity of each image frame. The average concentration field of N image frames is defined as:

$$\overline{I^*(x,y)} = \frac{\sum_{i=1}^{N+1} I^*_i(x,y)}{N} \quad (6)$$

where $\overline{I^*(x,y)}$ is the intensity matrix of each image frame. The mixing performance, which is the degree of disturbance, can be derived from the dispersion of the average field. The mean square perturbation field, $\overline{\sigma^*(x,y)^2}$:

$$\overline{\sigma^*(x,y)^2} = \frac{\sum_{i=1}^{N+1} \left[I^*_i(x,y) - \overline{I^*(x,y)} \right]^2}{N} \quad (7)$$

The extent of disturbance in the ROI is then evaluated by calculating the mean value of the intensity of the mean square perturbation field in this area:

$$DOP = \frac{\sum \overline{\sigma^*(x,y)^2}}{n} \quad (8)$$

where n is the total pixels in the ROI and DOP is the degree of perturbation and is used to assess the mixing performance. When there is no movement of the particles inside the liquid marble, the degree of perturbation is zero. The degree of perturbation will increase when perturbation occurs, with a maximum value of 1 when the perturbation happens in every pixel in the ROI. In our study, since one liquid marble can only accommodate a few number of particles, thus the degree of

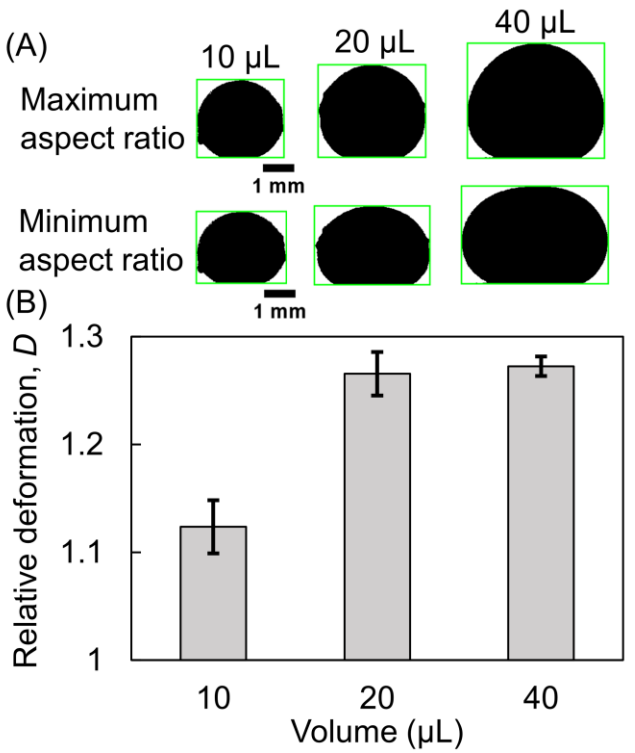

Figure 3. The deformation of liquid marbles as function of their volume. (A) Profile of liquid marble with different volume of 10, 20 and 40 µL at the largest and smallest aspect ratio position under a 385-kV/m electric field. (B) The relative deformation of a liquid marble versus volume.

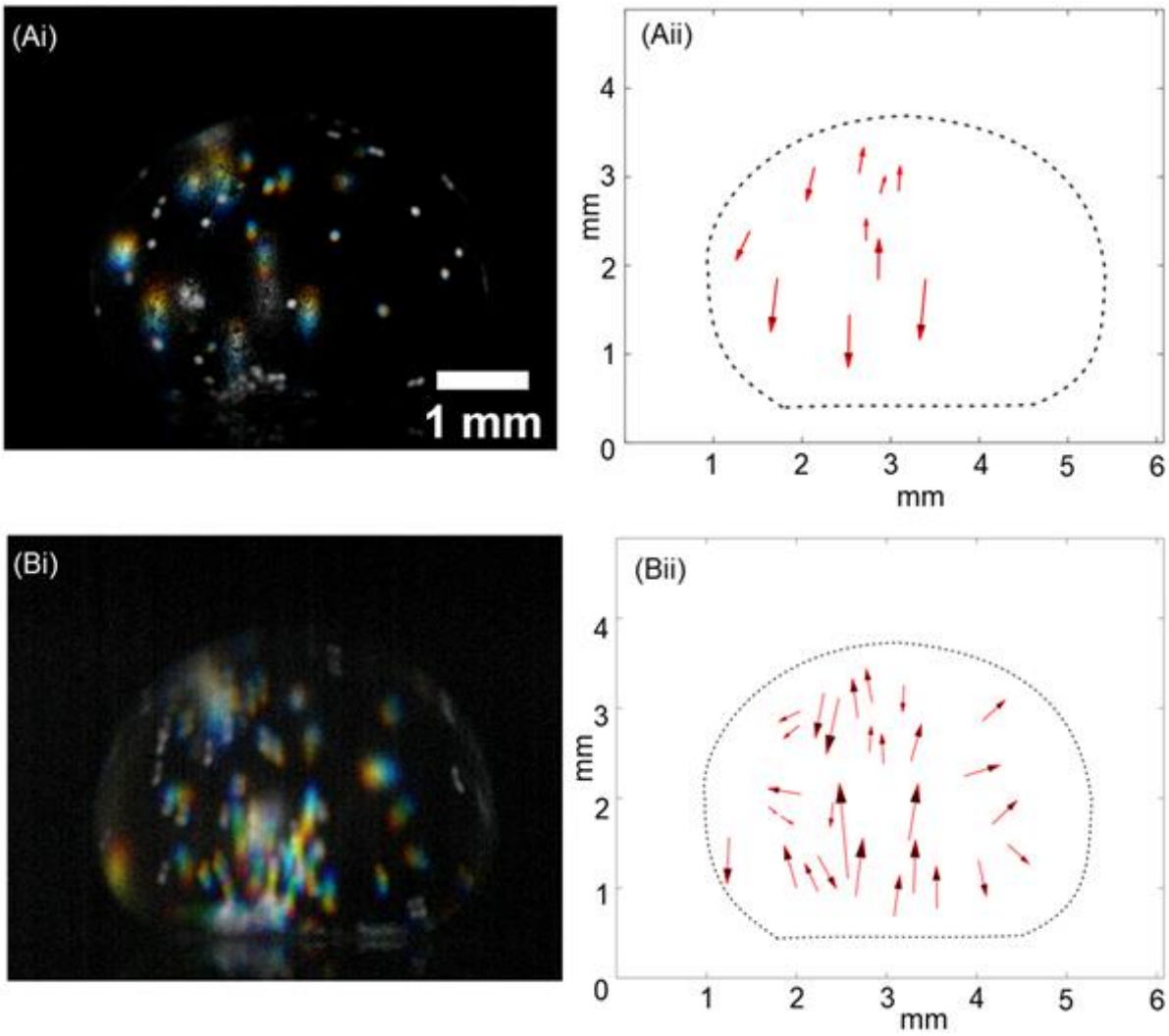

Figure 4. Movement of fluorescent particles inside 40-µL liquid marbles (Ai) without actuation and (Bi) with actuation under an AC electric field strength of 385 kV/m. For clarification, red arrows were added to indicate the direction and magnitude of the particle movement of the fluorescent particles over the investigated time period in subfigure (Aii) without actuation and (Bii) with actuation under an AC electric field strength of 385 kV/m.

perturbation in the ROI was limited. Therefore, we expect the degree of perturbation is larger than zero but much smaller than 1.

4. Results and discussion

This section discusses the use of an AC electric field to induce vibration and deformation of a liquid marble, which enhances the mixing performance. First, we discuss the natural frequencies of liquid marbles which is twice the input frequency used to actuate liquid marble at resonance in the subsequent experiments. The next sections report the deformation and mixing performance of liquid marble using this method.

4.1. Deformation of a liquid marble

The change of the liquid marble height over time under a pulse excitation was analysed using MATLAB. Fast Fourier Transform (FFT) was used to find the natural frequency of the liquid marble. For each trial, 1,024 (2^{10}) frames were analysed and the frequency with the largest magnitude was determined as the natural frequency of liquid marble. The natural frequencies of liquid marbles with a volume ranging from 10, 20, and 40 µL are determined as 47.57, 34.21 and 27. 37 Hz, respectively.

Figure 2(A) shows a liquid marble vibrating in an AC electric field. The vibration amplitude increased notably at higher electric field strength. Figure 2(B) indicates that the relative deformation increases with increasing electric field strength, rising from 1.12, 1.23, and 1.27 under an electric field of 153, 308 and 385 kV, respectively. Since the volume was kept constant at 40 µL, the gravitational force acting on the liquid marble was the same for all cases. The increase in relative deformation can be explained by the relationship between the electrostatic force acting on the liquid marble, which is proportional to E^2. Thus, the deformation becomes more profound as the electric strength increase.[37] Therefore, we

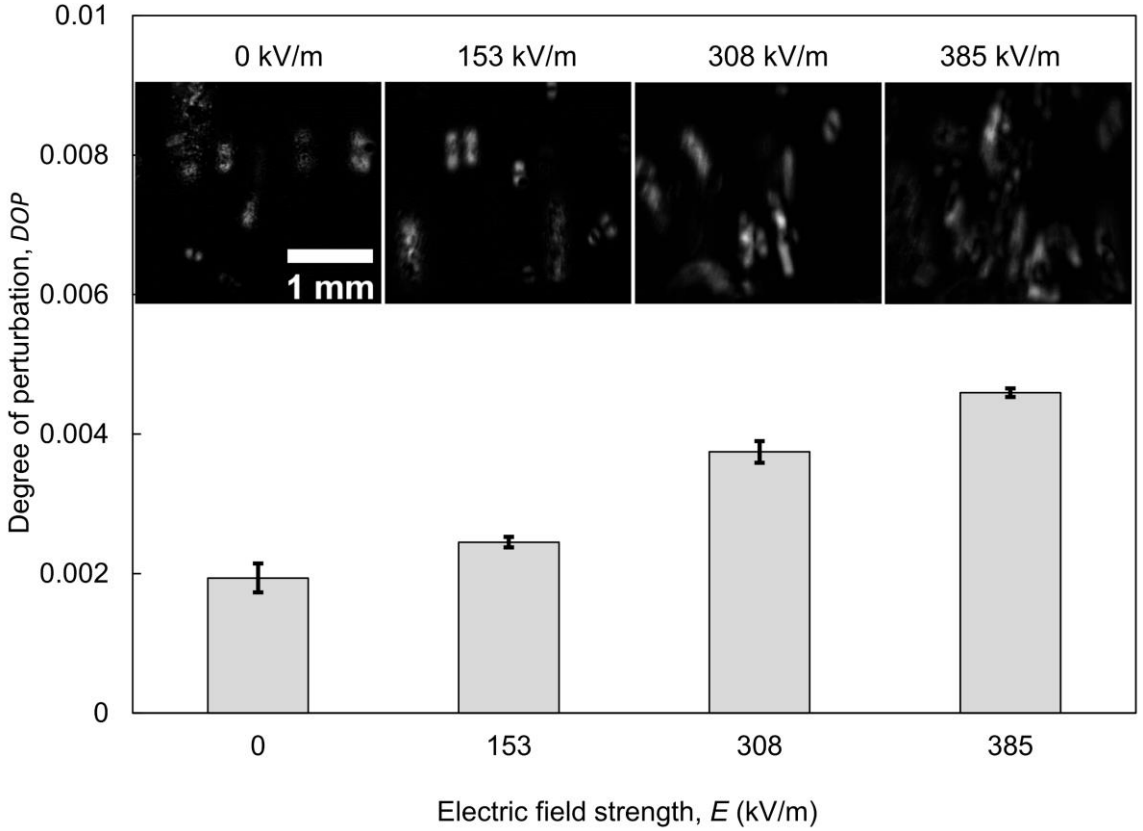

Figure 5. Degree of perturbation in the ROI of 40-µL liquid marbles under different electric field strengths. Images of the mean-square perturbation field with no actuation, 153, 308 and 385-kV/m electric field were exhibited above the graph.

expect a stronger electric field will deliver more significant mixing enhancement.

Figure 3(A) shows that the deformation of liquid marble varies depending on its volume. While the 10-µL liquid marble only experienced a small deformation, a more significant change in aspect ratio can be observed with the 20-µL and 40-µL liquid marble. The relative deformations of the three volumes are 1.12, 1.26 and 1.27, respectively, Figure 3(B). From 10 µL to 20 µL, the relative deformation increases notably while no significant difference was observed from 20 µL to 40 µL. The negligible change with a large volume can be caused by the larger mass and the more significant role of gravitational force relative to the electrostatic force.

4.2. Enhancement of mixing in a liquid marble

To understand and compare the movement of particles inside a liquid marble, we first selected image frames that correspond to the same duration of 8.5 seconds of a 40-µL liquid marble with and without actuation. Next, we changed the hue of the image frames so that the first image frame would have a red hue and gradually change to a blue hue at the last image frame. The image frames were then stacked together, allowing the observation of movement paths of the fluorescent particles as lines with a changing colour from red to blue, Figure 4. Furthermore, the magnitude and the direction of the particle displacement are depicted as a vector, which is equivalent to the velocity of the particle as determined with particle tracking velocimetry. Because the particle may move in and out of the image plane. We are cautious not to call these displacement vectors velocity vectors.

Figure 4 shows that more particles were dispersed throughout the liquid marble when it was excited. Non-moving particles were coloured white due to the stacking of image frames with a different hue from red to blue at the same position. While Figure 4(A) indicates that numerous particles are located at the bottom of the liquid marbles and not moving during the evaluation period, the particles in Figure 4(B) moved up due to the internal flow induced by the vibration and deformation of the liquid marble. It should be stressed that the excitation of the electric field was strong enough to disperse large-sized fluorescent particles used in this study, which is in the range of 90-105 µm. This mixing strategy thus has significant potential since it provides a means to perform reactions involving large-sized solid reactants or heterogeneous catalyst. The effect of electric field strength on the mixing performance was evaluated by comparing the degree of perturbation field in each case, Figure 5.

Figure 5 shows that all the degrees of perturbation are larger than zero, but much smaller than 1. However, the degree of perturbation of all the actuated liquid marbles was significantly higher than the non-actuated ones. A stronger degree of perturbation field indicates more advection in the ROI during the investigation period. This is expected due to the induced vibration and the deformation of the liquid marble under excitation. The stronger electric field delivers a higher mixing performance. The degree of perturbation under 385

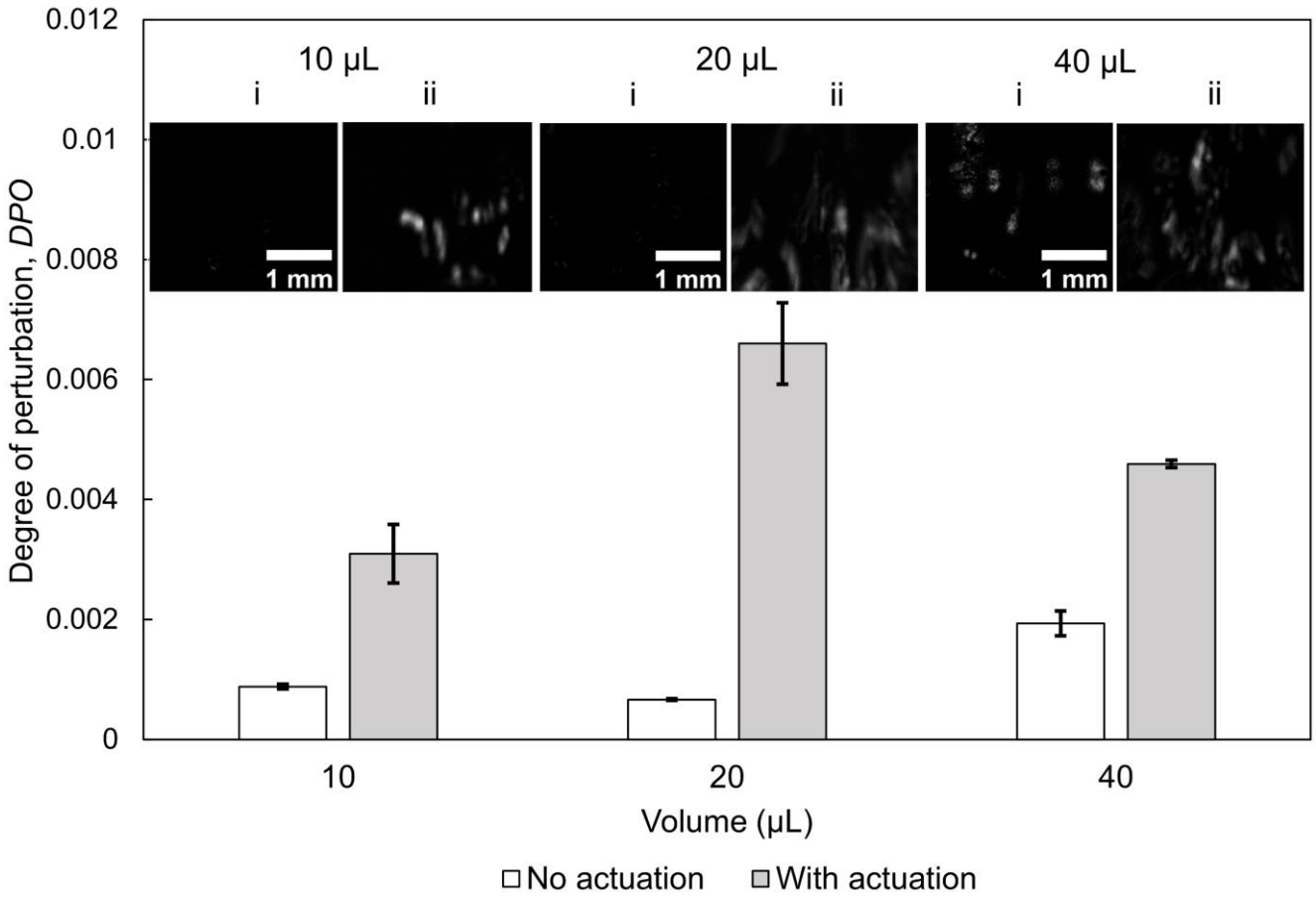

Figure 6. Degree of perturbation of in the ROI of liquid marbles with different volume of 10, 20 and 40 µL. Images of the mean-square perturbation field of liquid marbles with volume of 10, 20 and 40 µL with (i) no actuation and (ii) actuated under a 385-kV/m electric field.

kV/m is 1.88 and 2.33 times more than that under 153 kV/m and no-actuation, respectively. Images of the mean-square perturbation field in Figure 5 show that while only minor displacements in the vertical direction were achieved with actuation at 153 kV/m, the strong electric field strength of 308 and 385 kV/m caused noticeable displacements. This can be attributed to the larger vibration amplitude and deformation at a higher electric field strength, as reported in the previous section. These results also agree with the study of Lee et al. on the effect of increasing oscillating amplitudes and mixing performance. [67]

The enhancement of mixing performance with different liquid marble volumes is shown in Figure 6. Figure 6 also indicates that while there was almost no perturbation without actuation, the vibration and deformation induced by the electric field can lead to turbulence. For each liquid marble volume, the actuation of liquid marble always delivers more perturbation in the ROI, indicating an improvement in mixing performance. In particular, the degree of perturbation of an actuated liquid marble is more than 10 times that of a non-actuated 20-µL liquid marble. These results demonstrate the feasibility of using this mixing strategy for various liquid marble volumes. Our findings demonstrate that the electrostatic excitation of liquid marble could induce a strong internal forced convective flow which leads to enhanced mixing. The excitation is sufficiently strong to disperse large fluorescent particles, providing a promising mixing strategy for liquid marble-based platforms.

We studied the iodine–starch test to investigate the feasibility of applying this mixing strategy to liquid marble-based microreactors. A 19-µL liquid marble containing a starch solution with a concentration of 0.05% was injected with a volume of 1 µL of Lugol's iodine solution, thus forming a 20-µL liquid marble. The liquid marble was then actuated at resonance under a 385-kV/m electric field, Figure 7(A). As a benchmark, a similar reaction was carried out in a liquid marble with the same volume without actuation, Figure 7(B). The actuated liquid marble only required 30 seconds for the Lugol's iodine to completely diffuse and react with the starch, whereas the non-actuated liquid marble required 8 minutes. The reaction time is thus reduced by 16 times with this mixing strategy.

5. Conclusions

We demonstrated for the first time electrostatic excitation as an actuation scheme to enhance mixing in a liquid marble as a contactless and on-demand mean. The mixing performance

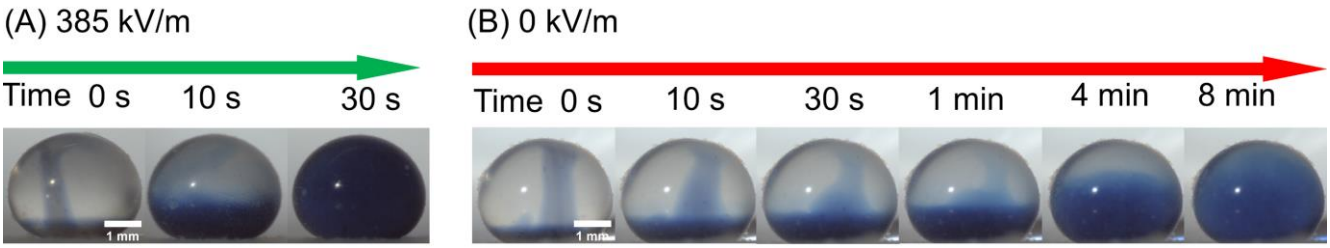

Figure 7. Starch-iodine reaction in a 20-µL liquid marble (A) actuated under a 385-kV/m electric field and (B) without actuation. Scale bar is 1mm.

was improved more than 10 times with an electric field of 385 kV/m. In a previous work by Ooi et al., the modelling indicated that even when a high voltage of 3,000 volts is applied to the liquid marble, the electric field within the liquid marble is negligible.[48] However, it is necessary to investigate the electric field inside the liquid marble and its effect on cells in future works. We also demonstrated the ability to disperse solid particles inside the liquid marble has immense benefits for microreaction applications involving large solid reactant particles or heterogeneous catalyst. Our method proved to be an effective mixing strategy that fills the gap of a contactless and on-demand mixing scheme on liquid marble. Since the mixing improvement mainly comes from the vibration and deformation of liquid marble, various manipulation schemes such as acoustic waves are also expected to be applicable.

Conflicts of interest

"There are no conflicts to declare".

Acknowledgements

C.H.O. acknowledges funding support from the Australian Research Council (ARC) Discovery Early Career Research Award (DECRA) DE200100119. N.T.N. acknowledges funding support from the ARC Discovery Project DP170100277. N.K.N. acknowledges funding support from the Griffith University International Postgraduate Research Scholarship and the ARC DECRA Postgraduate Research Scholarship.

Notes and references

1. B. K. Gale, A. R. Jafek, C. J. Lambert, B. L. Goenner, H. Moghimifam, U. C. Nze and S. K. Kamarapu, *Inventions*, 2018, **3**, 60.
2. N.-T. Nguyen, M. Hejazian, C. H. Ooi and N. Kashaninejad, *Micromachines*, 2017, **8**, 186.
3. K. i. Ohno, K. Tachikawa and A. Manz, *Electrophoresis*, 2008, **29**, 4443-4453.
4. N.-T. Nguyen, S. T. Wereley and S. A. M. Shaegh, *Fundamentals and applications of microfluidics*, Artech house, 2019.
5. D. J. Beebe, G. A. Mensing and G. M. Walker, *Annual review of biomedical engineering*, 2002, **4**, 261-286.
6. M. Mahmud, E. J. Blondeel, M. Kaddoura and B. D. MacDonald, *Micromachines*, 2018, **9**, 220.
7. K. S. Elvira, X. C. i Solvas, R. C. Wootton and A. J. Demello, *Nature chemistry*, 2013, **5**, 905.
8. W.-Y. Lin, Y. Wang, S. Wang and H.-R. Tseng, *Nano today*, 2009, **4**, 470-481.
9. J. Křenková and F. Foret, *Electrophoresis*, 2004, **25**, 3550-3563.
10. L. Capretto, W. Cheng, M. Hill and X. Zhang, in *Microfluidics: Technologies and Applications*, ed. B. Lin, Springer Berlin Heidelberg, Berlin, Heidelberg, 2011, DOI: 10.1007/128_2011_150, pp. 27-68.
11. A. Abou-Hassan, O. Sandre and V. Cabuil, *Angewandte Chemie International Edition*, 2010, **49**, 6268-6286.
12. C.-Y. Lee, C.-L. Chang, Y.-N. Wang and L.-M. Fu, *International journal of molecular sciences*, 2011, **12**, 3263-3287.
13. N.-T. Nguyen, *Micromixers: fundamentals, design and fabrication*, William Andrew, 2011.
14. N.-T. Nguyen and Z. Wu, Journal of Micromechanics and Microengineering, 2004, 15, R1-R16.
15. Y. Zhao and K. Chakrabarty, *IEEE transactions on computer-aided design of integrated circuits and systems*, 2012, **31**, 817-830.
16. L. Sicignano, G. Tomaiuolo, A. Perazzo, S. P. Nolan, P. L. Maffettone and S. Guido, *Chemical Engineering Journal*, 2018, **341**, 639-647.
17. E. Dressaire and A. Sauret, *Soft Matter*, 2017, **13**, 37-48.
18. P. Aussillous and D. Quéré, *Nature*, 2001, **411**, 924-927.
19. C. H. Ooi, R. Vadivelu, J. Jin, K. R. Sreejith, P. Singha, N.-K. Nguyen and N.-T. Nguyen, *Lab on a Chip*, 2021, **21**, 1199-1216.
20. S. Asare-Asher, J. N. Connor and R. Sedev, *Journal of Colloid and Interface Science*, 2015, **449**, 341-346.
21. Y. Rane, E. Foster, M. Moradiafrapoli and J. O. Marston, *Powder Technology*, 2018, **338**, 7-16.
22. C. H. Ooi, R. K. Vadivelu, J. St John, D. V. Dao and N.-T. Nguyen, *Soft Matter*, 2015, **11**, 4576-4583.
23. N.-T. Nguyen, *Micromachines*, 2020, **11**, 1004.
24. P. McEleney, G. M. Walker, I. A. Larmour and S. E. J. Bell, *Chemical Engineering Journal*, 2009, **147**, 373-382.
25. J. O. Castro, B. M. Neves, A. R. Rezk, N. Eshtiaghi and L. Y. Yeo, *ACS Applied Materials & Interfaces*, 2016, **8**, 17751-17756.
26. B. Wang, K. F. Chan, F. Ji, Q. Wang, P. W. Y. Chiu, Z. Guo and L. Zhang, *Advanced Science*, 2019, **6**, 1802033.
27. K. R. Liyanaarachchi, P. M. Ireland, G. B. Webber and K. P. Galvin, *Applied Physics Letters*, 2013, **103**, 054105.
28. C. A. Thomas, M. Kasahara, Y. Asaumi, B. T. Lobel, S. Fujii, P. M. Ireland, G. B. Webber and E. J. Wanless, *Soft Matter*, 2019, **15**, 7547-7556.
29. P. M. Ireland, C. A. Thomas, B. T. Lobel, G. B. Webber, S. Fujii and E. J. Wanless, *Journal of Physics: Conference Series*, 2019, **1322**, 012006.
30. P. Aussillous and D. Quéré, *Proceedings of the Royal Society A: Mathematical, Physical and Engineering Sciences*, 2006, **462**, 973-999.
31. P. Singha, C. H. Ooi, N.-K. Nguyen, K. R. Sreejith, J. Jin and N.-T. Nguyen, *Microfluidics and Nanofluidics*, 2020, **24**, 1-15.

32. P. Singha, N. K. Nguyen, K. R. Sreejith, H. An, N. T. Nguyen and C. H. Ooi, *Advanced Materials Interfaces*, 2021, **8**, 2001591.
33. C. H. Ooi, P. Singha, N.-K. Nguyen, H. An, V. T. Nguyen, A. V. Nguyen and N.-T. Nguyen, *Soft Matter*, 2021, **17**, 4069-4076.
34. C. Wang and Y. He, *Colloids and Surfaces A: Physicochemical and Engineering Aspects*, 2018, **558**, 367-372.
35. E. Bormashenko, *Current Opinion in Colloid & Interface Science*, 2011, **16**, 266-271.
36. Y. Xue, H. Wang, Y. Zhao, L. Dai, L. Feng, X. Wang and T. Lin, *Advanced materials*, 2010, **22**, 4814-4818.
37. D. Wang, L. Zhu, J. F. Chen and L. Dai, *Angewandte Chemie*, 2016, **128**, 10953-10957.
38. N.-K. Nguyen, C. H. Ooi, P. Singha, J. Jin, K. R. Sreejith, H.-P. Phan and N.-T. Nguyen, *Processes*, 2020, **8**, 793.
39. B. P. Mahadik, T. D. Wheeler, L. J. Skertich, P. J. Kenis and B. A. Harley, *Advanced healthcare materials*, 2014, **3**, 449-458.
40. Z. Liu, T. Yang, Y. Huang, Y. Liu, L. Chen, L. Deng, H. C. Shum and T. Kong, *Advanced Functional Materials*, 2019, **29**, 1901101.
41. Y. Lu, M. Zhang, H. Zhang, J. Huang, Z. Wang, Z. Yun, Y. Wang, W. Pang, X. Duan and H. Zhang, *Microfluidics and Nanofluidics*, 2018, **22**, 146.
42. M. Li, J. Tian, L. Li, A. Liu and W. Shen, *Chemical Engineering Science*, 2013, **97**, 337-343.
43. Z. Chen, D. Zang, L. Zhao, M. Qu, X. Li, X. Li, L. Li and X. Geng, *Langmuir*, 2017, **33**, 6232-6239.
44. K. Y. Lee, S. Park, Y. R. Lee and S. K. Chung, *Sensors and actuators A: Physical*, 2016, **243**, 59-65.
45. J. Jin, C. H. Ooi, K. R. Sreejith, D. V. Dao and N.-T. Nguyen, *Physical Review Applied*, 2019, **11**, 044059.
46. S. Mettu and M. K. Chaudhury, *Langmuir*, 2008, **24**, 10833-10837.
47. E. Bormashenko, R. Pogreb, T. Stein, G. Whyman, M. Schiffer and D. Aurbach, *Journal of adhesion science and technology*, 2011, **25**, 1371-1377.
48. C. H. Ooi, J. Jin, A. V. Nguyen, G. M. Evans and N.-T. Nguyen, *Microfluidics and Nanofluidics*, 2018, **22**, 1-9.
49. J. Jin, C. H. Ooi, K. R. Sreejith, J. Zhang, A. V. Nguyen, G. M. Evans, D. V. Dao and N.-T. Nguyen, *Microfluidics and Nanofluidics*, 2019, **23**, 1-9.
50. J. Jin, K. R. Sreejith, C. H. Ooi, D. V. Dao and N.-T. Nguyen, *Physical Review Applied*, 2020, **13**, 014002.
51. G. McHale, D. Herbertson, S. Elliott, N. Shirtcliffe and M. Newton, *Langmuir*, 2007, **23**, 918-924.
52. M. Newton, D. Herbertson, S. Elliott, N. Shirtcliffe and G. McHale, *Journal of physics D: Applied physics*, 2006, **40**, 20.
53. G. McHale, S. Elliott, M. Newton, D. Herbertson and K. Esmer, *Langmuir*, 2009, **25**, 529-533.
54. H. Suzuki and C.-M. Ho, 2002, *MEMS 2002 IEEE International Conference. Fifteenth IEEE International Conference on Micro Electro Mechanical Systems*, 40-43.
55. H. Gong, Y. Peng, H. Shang, Z. Yang and X. Zhang, *Chemical Engineering Science*, 2015, **128**, 21-27.
56. K. Rayat and F. Feyzi, *Fluid phase equilibria*, 2012, **316**, 156-163.
57. Y.-S. Shin and H.-C. Lim, *The European Physical Journal E*, 2014, **37**, 1-10.
58. J. S. Eow and M. Ghadiri, *Colloids and Surfaces A: Physicochemical and Engineering Aspects*, 2003, **219**, 253-279.
59. O. Fujii, K. Honsali, Y. Mizuno and K. Naito, *IEEE Transactions on Dielectrics and Electrical Insulation*, 2010, **17**, 566-571.
60. J. M. Oh, S. H. Ko and K. H. Kang, *Langmuir*, 2008, **24**, 8379-8386.
61. S. Dash, N. Kumari and S. V. Garimella, *Journal of Micromechanics and Microengineering*, 2012, **22**, 075004.
62. O. Fujii, K. Honsali, Y. Mizuno and K. Naito, *IEEE Transactions on Dielectrics and Electrical Insulation*, 2009, **16**, 116-122.
63. N.-K. Nguyen, P. Singha, J. Zhang, H.-P. Phan, N.-T. Nguyen and C. H. Ooi, *ChemPhysChem*, 2021, **22**, 99-105.
64. P. S. Bhosale, M. V. Panchagnula and H. A. Stretz, *Applied Physics Letters*, 2008, **93**, 034109.
65. J. H. Park, D. Hwang, J. Lee, S. Im and E. Kim, *Thin Solid Films*, 2007, **515**, 4041-4044.
66. J. D. Posner and J. G. Santiago, *Journal of Fluid Mechanics*, 2006, **555**, 1-42.
67. C.-P. Lee, H.-C. Chen and M.-F. Lai, *Biomicrofluidics*, 2012, **6**, 012814.